*in Proc. IEEE ICASSP-2002, Orlando (FL), May 2002. pp. 2549-2552.*

# ADAPTIVE PREDICTION OF TIME-VARYING CHANNELS FOR CODED OFDM SYSTEMS

*Dieter Schafhuber, Gerald Matz, and Franz Hlawatsch*

Institute of Communications and Radio-Frequency Engineering, Vienna University of Technology
Gusshausstrasse 25/389, A-1040 Vienna, Austria
phone: +43 1 58801 38973, fax: +43 1 58801 38999, email: dschafhu@aurora.nt.tuwien.ac.at
web: http://www.nt.tuwien.ac.at/dspgroup/time.html

## ABSTRACT

We propose adaptive channel predictors for orthogonal frequency division multiplexing (OFDM) communications over time-varying channels. Successful application of the normalized least-mean-square (NLMS) and recursive least-squares (RLS) algorithms is demonstrated. We also consider the use of adaptive channel predictors for delay-free equalization, thereby avoiding the need for regular transmission of pilot symbols. Simulation results demonstrate the good performance of the proposed techniques.

## 1. INTRODUCTION

*Orthogonal frequency division multiplexing* (OFDM) is an attractive modulation technique for high data-rate wireless communications [1]. A crucial issue in achieving high quality of service in wireless communications is reliable channel estimation [2, 3]. Beyond that, it was recently recognized that channel *prediction* is useful for various tasks like delay-free equalization, adaptive modulation, and power control [4–6].

Here, we propose two adaptive, decision-directed predictors for time-varying channels within a coded OFDM system. The adaptive channel predictors extend the minimum mean-square error (MMSE) channel predictor presented in [4]. We also propose a receiver structure in which the adaptive channel predictors are used for delay-free channel equalization without the use of pilot symbols.

This paper is organized as follows. The OFDM system is reviewed in Section 2. In Section 3, the MMSE channel predictor from [4] is extended to prediction horizon $p > 1$. The adaptive predictors are presented in Section 4 and applied to equalization in Section 5. Finally, simulation results are provided in Section 6.

## 2. OFDM SYSTEM MODEL

We consider an OFDM system with $K$ subcarriers. A block of bits $b[n,i]$, $i \in \{0,1,\ldots,B-1\}$ is encoded and mapped to transmit symbols denoted as $a[n,k]$. Here, $n \in \mathbb{Z}$ is the OFDM symbol (time) index and $k \in \{0,1,\ldots,K-1\}$ is the subcarrier (frequency) index. The $n$th OFDM symbol is obtained by applying an inverse discrete Fourier transform (IDFT) to the $a[n,k]$ and adding a cyclic prefix of length $L_{\mathrm{cp}}$,

$$s_n[m] = \begin{cases} \frac{1}{\sqrt{K}} \sum_{k=0}^{K-1} a[n,k]\, e^{j2\pi mk/K}, & m = -L_{\mathrm{cp}},\ldots,K-1, \\ 0, & \text{elsewhere.} \end{cases}$$

Thus, each OFDM symbol has length $N = K + L_{\mathrm{cp}}$. The overall transmit signal is $s[m] = \sum_{n=-\infty}^{\infty} s_n[m-nN]$.

Assuming a time-varying mobile radio channel with impulse response $h[m,l]$ ($l = 0,1,\ldots,L$, with $L \le L_{\mathrm{cp}}$ the maximum delay) and additive noise $\eta[m]$, the received signal is

$$r[m] = \sum_{l=0}^{L} h[m,l]\, s[m-l] + \eta[m]\,.$$

Funding by FWF grants P11904-TEC and P15156.

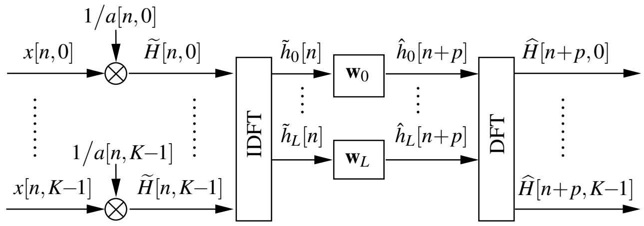


**Figure 1**: *Channel predictor structure.*

The noise $\eta[m]$ is assumed white and Gaussian with variance $\sigma_\eta^2$. The receiver discards the cyclic prefix and demodulates the received signal $r[m]$ by means of a DFT, which yields

$$x[n,k] = \frac{1}{\sqrt{K}} \sum_{m=0}^{K-1} r[nN+m]\, e^{-j2\pi km/K}.$$

It is assumed that the channel impulse response $h[m,l]$ varies negligibly within one symbol period. The input-output relation of the overall OFDM system can then be shown to equal

$$x[n,k] = H[n,k]\, a[n,k] + z[n,k]\,, \tag{1}$$

with the channel coefficients

$$H[n,k] = \sum_{l=0}^{L} h[nN,l]\, e^{-j2\pi kl/K}$$

and the noise

$$z[n,k] = \frac{1}{\sqrt{K}} \sum_{m=0}^{K-1} \eta[nN+m]\, e^{-j2\pi km/K}.$$

In what follows, the time-varying channel will be considered random. Under the *wide-sense stationary uncorrelated scattering* (WSSUS) assumption, the autocorrelation function of $h[m,l]$ is $\mathrm{E}\{h[m'+m,l]\, h^*[m',l']\} = r_h[m,l]\,\delta[l-l']$ [7, 8], and the channel's *Doppler spectra* or *scattering function* is defined as [7, 8]

$$S_h(\nu,l) = \sum_{m=-\infty}^{\infty} r_h[m,l]\, e^{-j2\pi\nu m}, \qquad l = 0,1,\ldots,L. \tag{2}$$

Here, $\nu$ is the normalized Doppler frequency.

## 3. MMSE CHANNEL PREDICTOR

Before considering adaptive predictors, we extend the MMSE channel predictor from [4] to prediction horizon $p > 1$. As was shown in [4], the MMSE predictor has the structure depicted in Fig. 1. It consists of divisions of the observations $x[n,k]$ by the transmit symbols $a[n,k]$, i.e.,

$$\widetilde{H}[n,k] = \frac{x[n,k]}{a[n,k]} = H[n,k] + \tilde{z}[n,k]\,, \tag{3}$$

where $\tilde{z}[n,k] = z[n,k]/a[n,k]$, followed by an IDFT, $L+1$ predictors, and a DFT. (For practical operation, the $a[n,k]$ are replaced with the symbols $\hat{a}[n,k]$ detected by the receiver.) The number of predictors equals the number of channel taps. The division in (3) is followed by an IDFT of $\widetilde{H}[n,k]$,

$$\tilde{h}_l[n] \;\triangleq\; \frac{1}{K}\sum_{k=0}^{K-1}\widetilde{H}[n,k]\,e^{j2\pi lk/K} = h_l[n] + \tilde{\eta}_l[n]\,, \qquad (4)$$

with the subsampled impulse response $h_l[n] \triangleq h[nN,l]$ and the noise samples $\tilde{\eta}_l[n] \triangleq \frac{1}{K}\sum_{k=0}^{K-1}\tilde{z}[n,k]\,e^{j2\pi lk/K}$.

In what follows, we assume random transmit symbols $a[n,k]$ that are stationary and white with respect to both $n$ and $k$. For each tap sequence, we consider a linear time-invariant predictor[1] of length $M$ with prediction horizon $p \geq 1$:

$$\hat{h}_l[n+p] = \mathbf{w}_l^H \tilde{\mathbf{h}}_l[n], \quad l = 0,1,\ldots,L, \qquad (5)$$

with the predictor filter $\mathbf{w}_l = [w_l[0], w_l[1], \ldots, w_l[M-1]]^T$ and the predictor input vector $\tilde{\mathbf{h}}_l[n] = [\tilde{h}_l[n], \tilde{h}_l[n-1], \ldots, \tilde{h}_l[n-M+1]]^T$. The predicted channel coefficients are then obtained as

$$\widehat{H}[n+p,k] = \sum_{l=0}^{L}\hat{h}_l[n+p]\,e^{-j2\pi kl/K}.$$

The predictor filters $\mathbf{w}_l$ are chosen to minimize the MSE

$$\begin{aligned}\varepsilon &\triangleq \frac{1}{K}\sum_{k=0}^{K-1}\mathrm{E}\big\{\big|H[n+p,k] - \widehat{H}[n+p,k]\big|^2\big\} \\ &= \sum_{l=0}^{L}\mathrm{E}\big\{\big|h_l[n+p] - \hat{h}_l[n+p]\big|^2\big\}\,. \qquad (6)\end{aligned}$$

Inserting (5) into (6) and using the orthogonality principle of linear MMSE estimation [9] yields the MMSE predictor filters

$$\mathbf{w}_{l,\mathrm{opt}} = \big(\mathbf{R}_h[l] + \beta\,\mathbf{I}\big)^{-1}\mathbf{r}_h^{(p)}[l]\,, \quad l = 0,1,\ldots,L. \qquad (7)$$

Here, $\mathbf{R}_h[l] \triangleq \mathrm{E}\big\{\mathbf{h}_l[n]\,\mathbf{h}_l^H[n]\big\}$ denotes the Hermitian Toeplitz $M \times M$ correlation matrix of the vector $\mathbf{h}_l[n] = [h_l[n], h_l[n-1], \ldots, h_l[n-M+1]]^T$. Furthermore, $\mathbf{r}_h^{(p)}[l] \triangleq \mathrm{E}\big\{\mathbf{h}_l[n]\,h_l^*[n+p]\big\} = \big[r_h[-pN,l],\, r_h[-(p+1)N,l], \ldots, r_h[-(p+M-1)N,l]\big]^T$ and $\beta \triangleq \sigma_\eta^2\,\mathrm{E}\big\{1/|a[n,k]|^2\big\}$. The MMSE can be shown to equal

$$\varepsilon_{\min} = \varepsilon\big|_{\mathbf{w}_l=\mathbf{w}_{l,\mathrm{opt}}} = \sum_{l=0}^{L}\big[r_h[0,l] - \mathbf{w}_{l,\mathrm{opt}}^H\mathbf{r}_h^{(p)}[l]\big]\,. \qquad (8)$$

Calculation of the MMSE channel predictor in (7) requires knowledge of the correlation function of the time-varying channel and the variance of the noise. In practice, these quantities would have to be estimated [10]. Even worse, since the statistics of real-world channels are stationary only over a certain time, they would have to be reestimated and the MMSE channel predictor would have to be recalculated once in a while. These problems are avoided by the adaptive channel predictors discussed next.

## 4. ADAPTIVE CHANNEL PREDICTORS

The adaptive channel predictors presented in this section perform a continual update of the predictor coefficients that replaces the explicit design (7). They do not assume knowledge of the channel and noise statistics and are capable of tracking nonstationary statistics. Assuming without loss of generality that the adaptation starts at $n = 0$, the predicted channel taps are (cf. (5))

$$\hat{h}_l[n+p] = \mathbf{w}_l^H[n]\,\tilde{\mathbf{h}}_l[n]\,, \quad n \geq 0,\; l = 0,1,\ldots,L,$$

with time-varying adaptive predictor filters $\mathbf{w}_l[n]$. We will apply two classical adaptation (update) algorithms, namely, the normalized least-mean-square (NLMS) algorithm and the recursive least-squares (RLS) algorithm.

[1] Using separate time-invariant predictor filters does not entail a loss of optimality since the channel is WSSUS and the noise is white [4].

**NLMS algorithm.** The NLMS algorithm belongs to the family of stochastic gradient algorithms and iteratively estimates the MMSE predictor filters [9]. We use the NLMS algorithm because the selection of the adaptation constant is simpler than for the LMS algorithm. The predictor filters $\mathbf{w}_l[n]$ are updated according to

$$\mathbf{w}_l[n] = \mathbf{w}_l[n-1] + \frac{\mu}{\|\tilde{\mathbf{h}}_l[n-p]\|^2}\,e_l^*[n]\,\tilde{\mathbf{h}}_l[n-p]\,, \quad n \geq p, \qquad (9)$$

where $\mu$ is the adaptation constant, $\|\tilde{\mathbf{h}}_l[n]\|^2 = \tilde{\mathbf{h}}_l^H[n]\,\tilde{\mathbf{h}}_l[n]$ is the power of the predictor input vector, and $e_l[n]$ is the prediction error given by

$$e_l[n] = h_l[n] - \mathbf{w}_l^H[n-1]\,\tilde{\mathbf{h}}_l[n-p]\,, \quad n \geq p. \qquad (10)$$

Since the true channel taps $h_l[n]$ are unavailable, we approximate them by the $\tilde{h}_l[n]$ in (4) and thus replace (10) with

$$e_l[n] \approx \tilde{h}_l[n] - \mathbf{w}_l^H[n-1]\,\tilde{\mathbf{h}}_l[n-p]\,, \quad n \geq p. \qquad (11)$$

The error introduced by this approximation will be small for practical signal-to-noise ratios (SNRs). Since the NLMS recursion in (9) starts with $n = p$, we initialize the prediction filters as

$$\mathbf{w}_l[n] = [1,0,\ldots,0]^T, \quad n = 0,1,\ldots,p-1.$$

Thus, $\hat{h}_l[n+p] = \tilde{h}_l[n]$ for $n = 0,1,\ldots,p-1$.

Stable operation requires $0 < \mu < 2$ [9]. The selection of $\mu$ is a trade-off between convergence speed and excess MSE. We obtained good results with $\mu \approx 0.5$.

**RLS algorithm.** With the RLS algorithm, the predictor coefficients $\mathbf{w}_l[n]$ are calculated such that they minimize the error [9]

$$\varepsilon_{\mathrm{RLS}}[n] \;\triangleq\; \sum_{i=p}^{n}\lambda^{n-i}\big|h_l[i] - \mathbf{w}_l^H[n]\,\tilde{\mathbf{h}}_l[i-p]\big|^2,$$

where $\lambda$ with $0 < \lambda \leq 1$ is a forgetting factor that accounts for possible nonstationarity of the input $\tilde{\mathbf{h}}_l[n]$ (we obtained good results for $\lambda = 0.99$). The resulting update equation for the predictor coefficients $\mathbf{w}_l[n]$ is

$$\mathbf{w}_l[n] = \mathbf{w}_l[n-1] + \mathbf{k}_l[n-p]\,e_l^*[n]\,, \quad n \geq p,$$

with $e_l[n]$ as in (11) and $\mathbf{k}_l[n]$ the RLS gain vector calculated as

$$\mathbf{k}_l[n] = \frac{\mathbf{P}_l[n-1]\,\tilde{\mathbf{h}}_l[n]}{\lambda + \tilde{\mathbf{h}}_l^H[n]\,\mathbf{P}_l[n-1]\,\tilde{\mathbf{h}}_l[n]}\,, \quad n \geq 1.$$

Here, $\mathbf{P}_l[n]$ is the inverse of the $M \times M$ matrix $\sum_{i=0}^{n}\lambda^{n-i}\,\tilde{\mathbf{h}}_l[i]\,\tilde{\mathbf{h}}_l^H[i]$; this inverse can be calculated recursively as

$$\mathbf{P}_l[n] = \frac{1}{\lambda}\Big(\mathbf{I} - \mathbf{k}_l[n]\,\tilde{\mathbf{h}}_l^H[n]\Big)\,\mathbf{P}_l[n-1]\,, \quad n \geq 1.$$

For initialization of the RLS recursion, we set

$$\begin{aligned}\mathbf{w}_l[n] &= [1,0,\ldots,0]^T, \quad n = 0,1,\ldots,p-1, \\ \mathbf{k}_l[0] &= \mathbf{P}_l[0]\,\tilde{\mathbf{h}}_l[0] = \frac{1}{\|\tilde{\mathbf{h}}[0]\|^2 + \delta}\,\tilde{\mathbf{h}}_l[0]\,, \\ \mathbf{P}_l[0] &= \big(\tilde{\mathbf{h}}_l[0]\,\tilde{\mathbf{h}}_l^H[0] + \delta\mathbf{I}\big)^{-1} = \frac{1}{\delta}\left[\mathbf{I} - \frac{\tilde{\mathbf{h}}_l[0]\,\tilde{\mathbf{h}}_l^H[0]}{\|\tilde{\mathbf{h}}[0]\|^2 + \delta}\right].\end{aligned}$$

Thus, $\hat{h}_l[n+p] = \tilde{h}_l[n]$ for $n = 0,1,\ldots,p-1$. The stabilization factor $\delta$ is in the range $0 < \delta \ll 1$ (we chose $\delta = 0.1$).

The RLS algorithm has a higher computational complexity than the NLMS algorithm. However, it has the advantages of faster convergence, small excess MSE, and a convergence rate that is independent of the eigenvalue spread of the input processes [9].

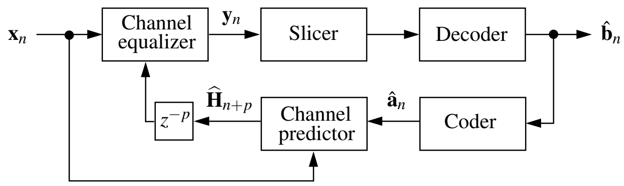


**Figure 2**: *OFDM receiver with predictive equalizer.*

## 5. OFDM RECEIVER WITH PREDICTIVE EQUALIZER

As mentioned in Section 1, channel prediction is useful for several tasks. An important example, delay-free equalization without the use of regular pilot symbols, will be considered in this section. Fig. 2 shows a block diagram of the proposed receiver [4]. The upper branch is a conventional OFDM receiver with equalizer. Based on the approximate input-output relation (1), the observed vector $\mathbf{x}_n = [x[n,0], x[n,1], \ldots, x[n,K-1]]^T$ is equalized according to

$$y[n,k] = \frac{x[n,k]}{\widehat{H}[n,k]}, \qquad k = 0,1,\ldots,K-1.$$

Here, the $\widehat{H}[n,k]$ are estimates of the current channel coefficients that are calculated by the lower branch. The equalized sequence $\mathbf{y}_n = [y[n,0], y[n,1], \ldots, y[n,K-1]]^T$ is then passed through a slicer and a decoder to obtain the (error-corrected) bits $\hat{\mathbf{b}}_n = [\hat{b}[n,0], \hat{b}[n,1], \ldots, \hat{b}[n,B-1]]^T$.

The lower branch of the receiver in Fig. 2 produces estimates $\widehat{\mathbf{H}}_{n+p} = [\widehat{H}[n+p,0], \widehat{H}[n+p,1], \ldots, \widehat{H}[n+p,K-1]]^T$ of the channel coefficients $H[n+p,k]$, to be used for equalization in a subsequent symbol interval (hence the delay by $z^{-p}$ in Fig. 2). The central part of the lower branch is an adaptive channel predictor as described in Section 4. The inputs of the channel predictor are the observed vector $\mathbf{x}_n$ and the estimated symbols $\hat{\mathbf{a}}_n = [\hat{a}[n,0], \hat{a}[n,1], \ldots, \hat{a}[n,K-1]]^T$ that are obtained by re-encoding the error-corrected detected bits $\hat{\mathbf{b}}_n$ (see Fig. 2). The prediction horizon $p$ is chosen to equal the decoding/re-encoding delay. Note that $\hat{\mathbf{a}}_n = \mathbf{a}_n$ only if all bit errors were corrected; otherwise, error propagation will result.

## 6. SIMULATION RESULTS

We simulated a coded OFDM system with $K = 120$ subcarriers, cyclic prefix length $L_{\rm cp} = 20$, and QPSK modulation with $|a[n,k]| = 1$. We used a $(15,7)$ Reed-Solomon (RS) code with each code symbol consisting of two QPSK symbols grouped in frequency. The RS code symbols were interleaved in frequency. The channel was simulated using the technique described in [11]. The scattering function (see (2)) of the simulated channel had a Jakes Doppler profile [7] and an exponentially decaying delay profile, i.e., $S_h(\nu,l) = (\nu_{\max}^2 - \nu^2)^{-1/2} \exp(-l/\tau_0)$ for $|\nu| < \nu_{\max}$ and $l = 0,\ldots,L$ and $S_h(\nu,l) = 0$ elsewhere. We chose $\tau_0 = L/\log_e(2L)$ and $L = 20$.

The channel predictor consisted of $L+1 = 21$ prediction filters (see Fig. 1), each of length $M = 10$. The prediction horizon was $p = 1$ unless indicated otherwise. The parameters of the NLMS and RLS algorithm were chosen as $\mu = 0.5$ and $\lambda = 0.99$, respectively.

**Convergence with ideal symbol feedback.** Fig. 3 shows the convergence of the adaptive channel predictors assuming ideal symbol feedback, i.e., without decoding errors. Both a "slow" channel ($\nu_{\max}K = 0.01$) and a "fast" channel ($\nu_{\max}K = 0.05$) are considered. The prediction MSE shown was estimated from 100 realizations. The estimated prediction MSE of the MMSE predictor from Section 3 and the theoretical MMSE in (8) are also plotted for comparison. The SNR $= \sum_l \int_\nu S(\nu,l)\, d\nu / \sigma_\eta^2$ was 15 dB. The adaptive predictors were initialized as explained in Section 4.

It is seen that the RLS algorithm converges rapidly with almost no excess MSE whereas the NLMS algorithm converges more slowly with an excess MSE of about 3 dB. For the slower channel, channel prediction is more accurate but convergence is slower (since for small $\nu_{\max}$ the channel taps are highly correlated).

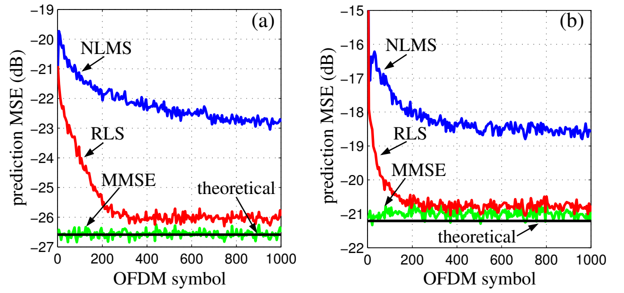


**Figure 3**: *Predictor convergence for ideal symbol feedback. (a) "Slow" channel, (b) "fast" channel.*

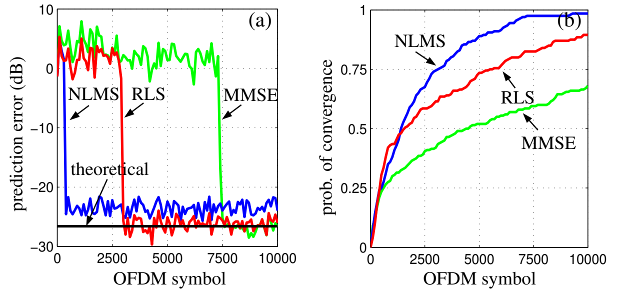


**Figure 4**: *Predictor convergence for decision-directed startup. (a) Squared prediction error for one realization, (b) estimated cumulative distribution function of the convergence time.*

**Convergence with decision-directed startup.** Next, we study the behavior of the channel predictors for decision-directed startup. (At initial time $n = 0$ a randomly selected OFDM symbol was used in (3).) Fig. 4(a) shows the temporal evolution of the squared prediction errors of the various predictors for one realization. Fig. 4(b) shows the cumulative distribution function (estimated from 200 realizations) of the convergence time for SNR $= 15$ dB. (The convergence time is the time the prediction MSE requires to fall below $-13$ dB.) It can be seen that for decision-directed startup, on average, the NLMS algorithm converges more rapidly than the RLS algorithm. Note that the MMSE filter is fixed; its prediction error behavior is due to decoding errors and error propagation.

**Channel predictability.** Fig. 5 shows how the prediction MSE after convergence depends on the prediction horizon $p$. Ideal symbol feedback was used. The MSE was estimated by averaging over 100 realizations with $10^4$ symbols each. The SNR was 25 dB. For the "slow" channel ($\nu_{\max}K = 0.01$) shown in Fig. 5(a), the prediction MSE obtained with the NLMS and RLS algorithm is below $-15$ dB for horizons up to 8 and 15 symbol periods, respectively. For the "fast" channel ($\nu_{\max}K = 0.05$) shown in Fig. 5(b), the prediction MSE is below $-15$dB for horizons up to 2 and 4 symbol periods, respectively. It can also be seen that the excess MSE of the NLMS algorithm increases rapidly with $p$ whereas the RLS algorithm nearly obtains the theoretical MMSE for all $p$ considered.

**Tracking of nonstationary channel statistics.** The ability of the adaptive channel predictors to track nonstationary channel statistics is studied in Fig. 6. Two different channels were generated: channel 1 has a constant scattering function (uniform Doppler and delay profile) for $|\nu| < \nu_{\max}$ and $l = 0,\ldots,L$, with $\nu_{\max}K = 0.01$ and $L = 15$; channel 2 has the Jakes-exponential scattering function used previously, with $\nu_{\max}K = 0.03$ and $L = 20$. We used channel 1 for the first 1000 OFDM symbols and channel 2 for the last 1000 OFDM symbols; for the intermediate transition period (corresponding to $n = 1001,\ldots,2000$), the channel was constructed by linearly interpolating between channel 1 and channel 2.

Fig. 6 shows the prediction MSE (estimated from 100 realizations) of the adaptive channel predictors for decision-directed oper-

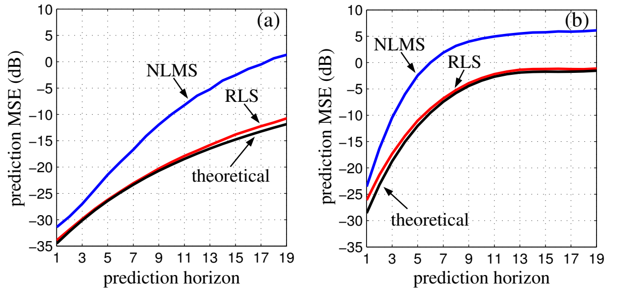


**Figure 5**: *Dependence of prediction accuracy on the prediction horizon p for (a) a "slow" channel and (b) a "fast" channel.*

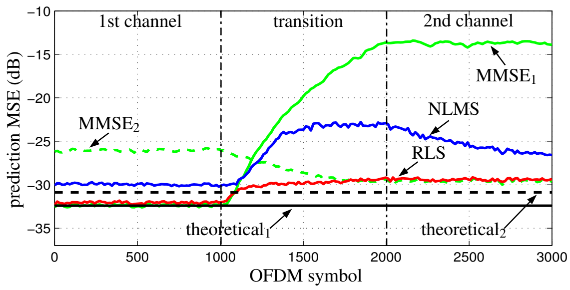


**Figure 6**: *Tracking of a channel with nonstationary statistics. The curves labeled MMSE$_1$ and MMSE$_2$ show the estimated prediction MSE of the MMSE predictor designed for channel 1 and 2, respectively. The curves labeled theoretical$_1$ and theoretical$_2$ show the theoretical MMSE for channel 1 and 2, respectively.*

ation (the initial convergence to channel 1 is not shown). It is seen that during each stationary period, the RLS algorithm performs as well as the respective MMSE predictor and nearly achieves the theoretical MMSE. The RLS algorithm is also good at tracking the nonstationary channel statistics during the transition period. The tracking results of the NLMS algorithm are much poorer, with a relatively high MSE during and even after the transition period.

**Receiver performance.** Finally, we study the performance of the OFDM receiver proposed in Section 5 (see Fig. 2) using the various channel predictors in decision-directed mode. The channel has the Jakes-exponential scattering function used previously, with $L = 20$ taps. Fig. 7(a) shows the prediction MSEs (estimated by averaging over 10 realizations with $10^4$ symbols each) of the MMSE, NLMS, and RLS algorithms for a "slow" channel ($\nu_{\max}K = 0.01$). The theoretical MMSE (8) and the MSE using pilot symbol assisted (PSA) channel estimation [12] are also shown for comparison. For PSA channel estimation, approximately 10% of the transmitted symbols were used as pilots. Due to the decision-directed operation, a threshold SNR is necessary for good performance of the predictors. For sufficiently high SNR, the predictors outperform PSA channel estimation and both the MMSE and the RLS predictors achieve the theoretical optimum. Again, the NLMS algorithm performs slightly worse and has about 3 dB excess MSE.

Fig. 7(c) shows the bit error rates (BERs) after the channel decoder for the "slow" channel when the result of channel prediction is used for equalization. The BERs of a "genius" receiver knowing the true channel and of a receiver using PSA channel estimation are also shown for comparison. Above the threshold SNR, the performance of all receivers is very similar; this is due to the relatively robust QPSK modulation. Fig. 7(b) and Fig. 7(d) show the prediction MSEs and BERs for a "fast" channel ($\nu_{\max}K = 0.05$). Generally speaking, the performance is worse than for the "slow" channel; in particular, the threshold SNR is about 2 dB higher. Note that with PSA channel estimation the effective data rate is significantly reduced.

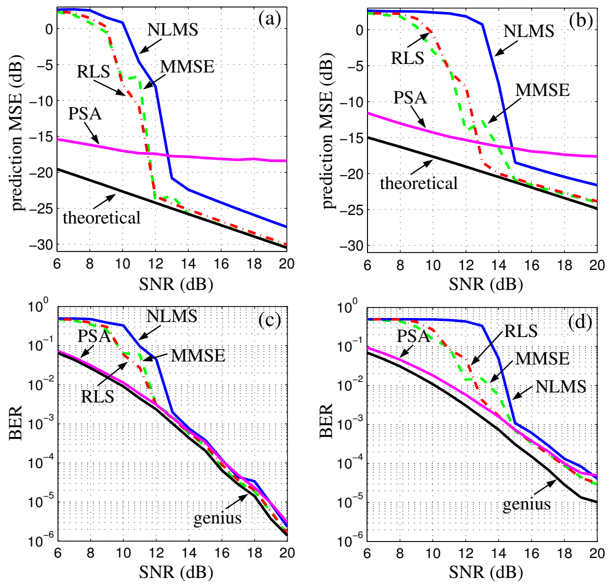


**Figure 7**: *Performance of the various receivers. (a) Prediction MSE for a "slow" channel, (b) prediction MSE for a "fast" channel, (c) BER for the "slow" channel, (d) BER for the "fast" channel.*

## 7. CONCLUSIONS

We developed adaptive channel predictors for OFDM transmission over time-varying mobile radio channels. The adaptive predictors do not require knowledge of the channel and noise statistics. With the RLS algorithm, almost optimum performance can be achieved. The NLMS algorithm has poorer performance but lower computational complexity.

## REFERENCES

[1] J. A. C. Bingham, "Multicarrier modulation for data transmission: An idea whose time has come," *IEEE Comm. Mag.*, vol. 28, pp. 5–14, May 1990.

[2] Y. Li, L. Cimini, and N. Sollenberger, "Robust channel estimation for OFDM systems with rapid dispersive fading channels," *IEEE Trans. Comm.*, vol. 46, pp. 902–915, July 1998.

[3] O. Edfors, M. Sandell, J.-J. van de Beek, S. K. Wilson, and P. O. Börjesson, "OFDM channel estimation by singular value decomposition," *IEEE Trans. Comm.*, vol. 46, pp. 931–939, July 1998.

[4] D. Schafhuber, G. Matz, and F. Hlawatsch, "Predictive equalization of time-varying channels for coded OFDM/BFDM systems," in *Proc. IEEE GLOBECOM-2000*, (San Franscisco, CA), pp. 721–725, Nov. 2000.

[5] F. Duel-Hallen, S. Hu, and H. Hallen, "Long-range prediction of fading signals," *IEEE Signal Processing Magazine*, vol. 17, pp. 62–75, May 2000.

[6] C. Y. Wong, R. S. Cheng, K. B. Letaief, and R. D. Murch, "Multiuser OFDM with adaptive subcarrier, bit, and power allocation," *IEEE J. Sel. Areas Comm.*, vol. 17, pp. 1747–1758, Oct. 1999.

[7] W. C. Jakes, *Microwave Mobile Communications*. New York: Wiley, 1974.

[8] P. A. Bello, "Characterization of randomly time-variant linear channels," *IEEE Trans. Comm. Syst.*, vol. 11, pp. 360–393, 1963.

[9] S. Haykin, *Adaptive Filter Theory*. Englewood Cliffs (NJ): Prentice Hall, 1991.

[10] H. Artés, G. Matz, and F. Hlawatsch, "Unbiased scattering function estimation during data transmission," in *Proc. IEEE VTC-99 Fall*, (Amsterdam, The Netherlands), pp. 1535–1539, Sept. 1999.

[11] D. Schafhuber, G. Matz, and F. Hlawatsch, "Simulation of wideband mobile radio channels using subsampled ARMA models and multistage interpolation," in *11th IEEE Workshop on Statistical Signal Processing*, (Singapore), pp. 571–574, Aug. 2001.

[12] Y. Li, "Pilot-symbol-aided channel estimation for OFDM in wireless systems," *IEEE Trans. Veh. Technol.*, vol. 49, pp. 1207–1215, July 2000.